Efficient Design of a Magneto-Rheological Fluid Embedded Pneumatic Vibration Isolator Considering Practical Constraints

Xiaocong ZHU* Xingjian JING* and Li CHENG*
*Department of Mechanical Engineering, Hong Kong Polytechnic University,
Hung Hom, Kowloon, Hong Kong, China
{mmzhuxc, mmjxj, mmlcheng}@polyu.edu.hk

Abstract
An efficient systematic design of a magneto-rheological fluid embedded pneumatic vibration isolator (MrEPI) considering practical constraints is proposed. The design is accomplished from three aspects including system level design for synthesizing appropriate non-dimensional system parameters of pneumatic spring and MR damping elements through performance sensitivity analysis considering compact and efficient hardware utilization, component level design for synthesizing optimal design of the MR valve through employing an objective function with preset index for guaranteeing required worst-case performance, and dimensional realization level design for determining actual plant parameters from aforementioned level designs according to practical constraints. In addition, the vibration control performance of the optimally designed MrEPI system under harmonic disturbances is evaluated, which shows good isolation performance under different stiffness.

Key words: Magneto-rheological Fluid, Pneumatic Isolator, Design, Practical Constraint

1. Introduction

Vibration isolators have been widely used for vibration suppression and isolation [1,2]. Compare to passive vibration isolators, semi-active and active vibration isolators could achieve prior isolation performance due to adjustable damping and/or stiffness and arbitrary force control. Specially, it is noted that a vibration isolator with independent control of stiffness and damping will have promising application in various vehicle suspension under different road requirements, advanced landing gear system for soft and hard landing, combined device of shock and vibration etc. [1-4].

Recently, a magneto-rheological fluid embedded pneumatic vibration isolator (MrEPI) allowing independently adjustable stiffness, damping and height control with hybrid and compact connection of pneumatic spring and MR damping elements was developed for vibration isolation application, and the advantage dynamic performance of system has been demonstrated through developing a nonlinear non-dimensional dynamic model with the full considerations of nonlinear pneumatic spring element and MR damping element [3]. Thereafter, it is necessary to develop a systematic design procedure for further practical usage of the MrEPI. However, the design of the MrEPI is very complex due to various and coupling design parameters in pneumatic cylinder and MR valve inducing hard analysis of achievable performance and relevant sensitivity. Moreover, the systematic and unified design process with practical constraints for the MrEPI should be extensively considered, which could possibly be accomplished through non-dimensional analysis regardless of

concrete system configuration and subsequent dimensional realization according to different application requirements.

It is noted that the optimal design of dual-chamber pneumatic isolator or air spring, which is an important part of the MrEPI, mostly focus on the orifice or capillary tube damping and volume ratio parameters of dual-chamber [5-7]. However, there are few comments about the optimal design of nonlinearity degree and pressure ratio of a nonlinear pneumatic vibrator, which seems to have obvious influence on the achievable performance [3]. On the other hand, the optimal design of a MR valve especially the volume constrained optimization of MR valve, which is an important damping component for the MrEPI, has also developed to some extends recently [8-10]. However, it is noted that the conventional multi-objective function utilized in the literature has unclear weight selections and has seldom consideration of practical constraints directly from application requirements. In addition, the minimum damping ratio for good isolation performance at high frequency is rarely well guaranteed in optimization procedure [11]. Therefore, an improved optimal design for the MR valve fulfilling practical constraints is necessarily developed.

2. Schematic Structure and Modeling of the MrEPI

The schematic structure of the MrEPI is shown in Fig.1. It consists of three low chambers filled with air gas (CG1,CG2,CG3) and two upper chambers filled with MR fluids (CM1, CM2). Chamber CG1 and CG2, functioning as a dual-working-chamber pneumatic spring to provide adjustable stiffness and height control, are separated by a moving piston with diaphragm seals and controlled by four pneumatic high speed on-off valves. An auxiliary chamber CG3 is connected to Chamber CG2 with a flow restrictor that is designed to operate on a laminar flow region for linear damping. A MR valve is connected to the two sides of a double-rod cylinder filled with MR fluids to provide adjustable damping.

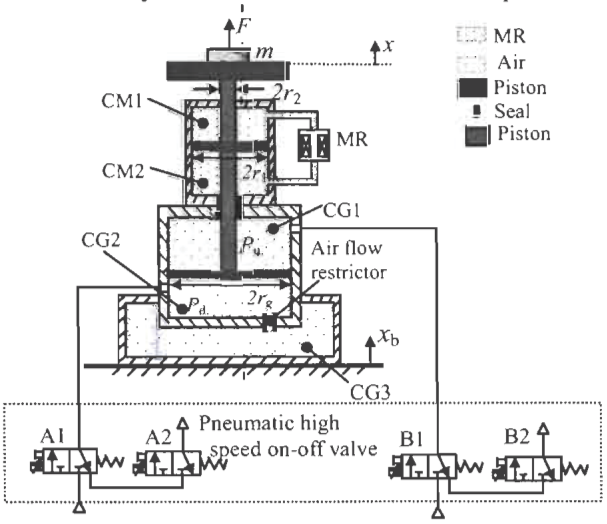

Fig. 1 The schematic structure of the MrEPI

The non-dimensional analytical models have been presented [3]:

$$\begin{cases} \dfrac{d^2\phi_x}{d\phi_t^2} = \dfrac{\phi_L}{\lambda}\left\{(1+\phi_{P01})\left[\dfrac{\phi_L(1+\phi_{V01})}{\phi_L(1+\phi_{V01})+\phi_x-\phi_{xm}}\right]^{\kappa}-1\right\} - s_{a2}\phi_{KP2}\dfrac{\phi_L}{\lambda}\left[\dfrac{\phi_{KL2}\phi_L(1+\phi_{V02})}{\phi_{KL2}(1+\phi_{V02})-(\phi_x-\Phi_{xb})}\right]^{\kappa} - F_{dn2}(\phi_x-\Phi_{xb},\dfrac{d\phi_x}{d\phi_t}-\dfrac{d\Phi_{xb}}{d\phi_t})+\Phi_F \\ \dfrac{\phi_L}{\lambda}\left\{(1+\phi_{P01})\left[\dfrac{\phi_L(1+\phi_{V01})}{\phi_L(1+\phi_{V01})+\phi_x-\phi_{xm}}\right]^{\kappa}-1\right\} = \dfrac{\phi_L}{\lambda}\left\{(1+\phi_{P03})\left[\dfrac{\phi_L(1+\phi_{V03})}{\phi_L(1+\phi_{V03})+\phi_{xm}-\Phi_{xb}}\right]^{\kappa}-1\right\} - 2\xi_3(\dfrac{d\phi_{xm}}{d\phi_t}-\dfrac{d\Phi_{xb}}{d\phi_t}) \end{cases} \quad (1)$$

Where, ϕ_x and ϕ_{xp} are the absolute and relative displacement of table top respectively. $\phi_L, \phi_{V0}, \phi_{P0}, \phi_{KP}, \phi_{KL}$ and ξ, ϕ_{DVMR} are the non-dimensional adjustable variables related to each pneumatic spring element or each MR damping element (including passive viscous damping). Φ_{xb} and Φ_F are the sinusoidal base and force excitation, respectively.

3. Design of the MrEPI with Practical Constraints

An effect systematic design procedure for the MrEPI considering practical constraints will be developed in the following, which consists of system level design for appropriately specifying non-dimensional design parameters of pneumatic spring and MR damping element, component level design for providing optimal non-dimensional parameters of the MR valve, and dimensional realization level design for obtaining actual plant parameters according to practical application requirements.

3.1 System Level Design

3.1.1 Natural frequency of the system

The output force of the MrEPI under harmonic piston motion is given according to Eq.(1)

$$F_n(\Omega)=\frac{\phi_L}{\lambda}\left\{(1+\phi_{P01})\left[\frac{1}{1+\frac{\phi_x(\Omega)-\phi_m(\Omega)}{\phi_L(1+\phi_{V01})}}\right]^{\lambda}-1\right\}-s_{u2}\phi_{KP2}\frac{\phi_L}{\lambda}\left[\frac{1}{1-\frac{\phi_x(\Omega)-\Phi_{xb}(\Omega)}{\phi_{KL2}\phi_L(1+\phi_{V02})}}\right]^{\lambda}-F_{dh2}(\phi_x-\Phi_{xb},j\Omega(\phi_x-\Phi_{xb})) \quad (2)$$

Where Ω is the non-dimensional excitation frequency.

The linearized complex equivalent stiffness of the entire system with hybrid connection of pneumatic spring elements could be given through utilizing linearization method to Eq.(2), which is used to quantitatively characterize the viscoelastic behavior of the isolator.

$$K^*=-\frac{\delta F_n}{\delta[\phi_x(\Omega)-\Phi_{xb}(\Omega)]}=\left[\frac{1+\phi_{P01}+2\xi_3 j\Omega(1+\phi_{V03})}{2+\phi_{V01}+\phi_{V03}+2\xi_3 j\Omega(1+\phi_{V01})(1+\phi_{V03})}+\frac{s_{u2}\phi_{KP2}}{\phi_{KL2}(1+\phi_{V02})}\right]=K'+jK''=K'(1+j\eta_{lost}) \quad (3)$$

The linearized equivalent spring stiffness and loss stiffness is derived from Eq.(3)

$$K'=\frac{(1+\phi_{P01})^3(2+\phi_{V01}+\phi_{V03})+4\xi_3^2(1+\phi_{P01})(1+\phi_{V01})(1+\phi_{V03})^2\Omega^2}{(1+\phi_{P01})^2(2+\phi_{V01}+\phi_{V03})^2+4\xi_3^2(1+\phi_{V01})^2(1+\phi_{V03})^2\Omega^2}+\frac{s_{u2}\phi_{KP2}}{\phi_{KL2}(1+\phi_{V02})}, \quad (4a)$$

$$K''=\frac{(1+\phi_{V01})^2(1+\phi_{V03})(2+\phi_{V01}+\phi_{V03})-(1+\phi_{P01})(1+\phi_{V01})(1+\phi_{V03})}{(1+\phi_{V01})^2(2+\phi_{V01}+\phi_{V03})^2+4\xi_3^2(1+\phi_{V01})^2(1+\phi_{V03})^2\Omega^2}2\xi_3\Omega \quad (4b)$$

In the above analysis, the nonlinear degree ϕ_L is not concluded in the formulation of complex stiffness due to linearization approximation. For more accurately evaluating the complex stiffness incurred by nonlinear degree ϕ_L. Alternatively, the nonlinearized complex stiffness K' and K'' could be calculated through supposing the isolator system being suffering harmonic displacement excitation $x(t)$ and the linearized viscoelastic force $f(t)$ from $F_n(\Omega)$ being calculated through Fourier series [13]. The linearized complex stiffness and nonlinearized complex stiffness will be employed for determining the appropriate configuration of ϕ_L and ξ_3 later.

Subsequently, the non-dimensional angular natural frequency is

$$\omega_n=\sqrt{\frac{K'}{m}}=\sqrt{\frac{(1+\phi_{P01})^3(2+\phi_{V01}+\phi_{V03})+4\xi_3^2(1+\phi_{P01})(1+\phi_{V01})(1+\phi_{V03})^2\Omega^2}{(1+\phi_{P01})^2(2+\phi_{V01}+\phi_{V03})^2+4\xi_3^2(1+\phi_{V01})^2(1+\phi_{V03})^2\Omega^2}+\frac{s_{u2}\phi_{KP2}}{\phi_{KL2}(1+\phi_{V02})}}, \quad (5)$$

As seen, the adjustable stiffness related to the natural frequency is dependent on several non-dimensional parameters ϕ_{V01}, ϕ_{P01}, ξ_3 and ϕ_L. Next, these parameters upon achievable performance will be analyzed and appropriate parameters will be given.

3.1.2 Specification of ϕ_L and ξ_3 for Pneumatic Spring

The required volume of pneumatic chamber is strongly dependent on the nonlinearity degree ϕ_L since the total volume is calculated as $V_t=\phi_L\hat{x}_{b0}[3+\phi_{V01}+\phi_{V03}]$ ($\hat{x}_{b0}$ is the maximum excitation amplitude). Therefore, it is appreciable to employ small ϕ_L for compact isolator design. However, when ϕ_L is small, there is more sever and unsatisfactory nonlinear behavior bringing about deteriorated isolation performance [3]. Fortunately, the unsatisfactory behavior could be improved through introducing the viscous

damping ξ_3 generated by air restrictor. As such, ϕ_L and ξ_3 should be designed first for achieving small gas volume and good isolation performance as much as possible.

It is noted that the loss factor is useful for evaluating resonance attenuation [6]. Fig.2 shows the comparison of linearized and nonlinearized loss factor for the MrEPI under different ξ_3 with same small $\phi_L = 3$ and under different ϕ_L with the same ξ_3. As seen from Fig.2a, the loss factor is initially increased and then decreased when excitation frequency is always increasing. It is noted that the linearized loss factor is almost equal to the nonlinearized loss factor only if ξ_3 is moderately specified ($\xi_3 \geq 0.25$) while there is great difference between two loss factor under too small ξ_3, which will induce severe unsatisfactory nonlinearity such as superharmonic, and too large ξ_3 will deteriorate the isolation performance at high frequency. Therefore, the appropriate ξ_3 could be $\xi_3 \approx 0.25$ for effectively removing unsatisfactory nonlinear behaviors of pneumatic spring without scarifying compact volume design purpose, as seen from Fig.2b. Fig 3 show the dynamic isolation performance of the MrEPI under different ϕ_L with the same ξ_3. As seen, the transmissibility of the MrEPI is almost the same while the force-mobility shows slight difference under different ϕ_L with the same ξ_3, indicating that ϕ_L could be set considerably small with a little large stiffness incurred and no significant deterioration of resonance attenuation and high frequency mitigation as long as appropriate ξ_3 is specified.

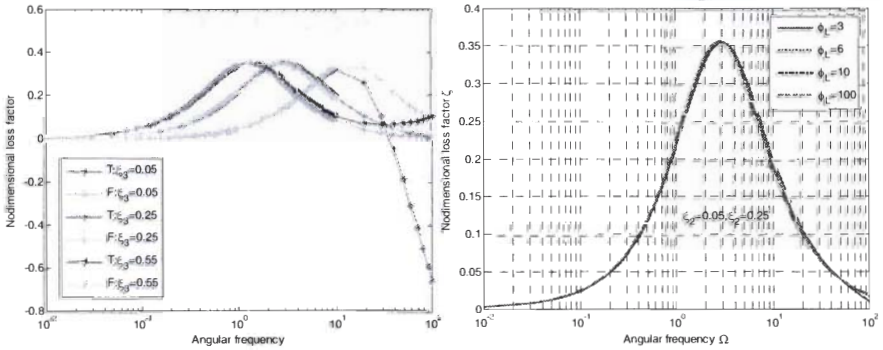

(a) under different ξ_3 with same ϕ_L (b) under different ϕ_L with same ξ_3

Fig 2 loss factor of the MrEPI

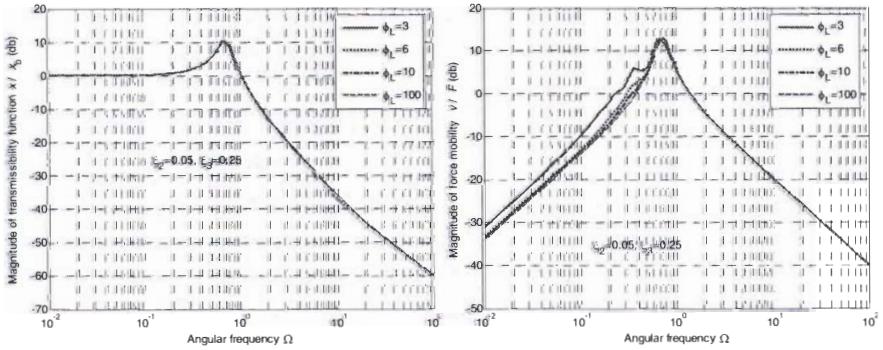

Fig 3 Isolation performance of the MrEPI under different ϕ_L and the same ξ_3

3.1.3 Specification of ϕ_{V0} for Pneumatic Spring

The additional volume ratio ϕ_{V0} is used to adjust the stiffness related to the natural frequency. According to Eq.(5), the relationship of the non-dimensional natural frequency ω_n and additional volume ratio ϕ_{V0} is shown in Fig.4. As seen, ω_n is decreased rapidly when ϕ_{V0} is increased slightly. And ω_n is gradually growing when ϕ_{V0} is increasing greatly. Thus, it is favorably to choose $\phi_{V0} = 4 \sim 5$ since ω_n can be down to 0.4 in this case and too large additional volume ratio has slightly influence on the natural frequency.

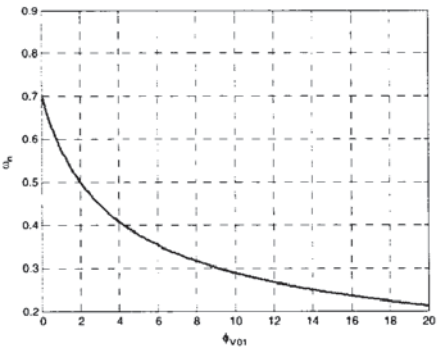

Fig 4 Relationship of natural frequency and ϕ_{V0}

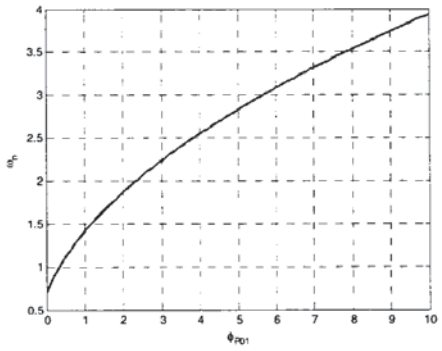

Fig.5 Relationship of natural frequency and ϕ_{P01}

3.1.4 Specification of ϕ_{P0} for pneumatic spring

(1) Permissible pressure ratio for variable stiffness adjustment

The additional pressure ratio ϕ_{P0} along with the same value of ϕ_{KP} is utilized to adjust system stiffness related to the natural frequency of the system. According to Eq.(5), the relationship of non-dimensional natural frequency ω_n and additional pressure ratio ϕ_{P0} is shown in Fig.5. As seen, ω_n is increased significantly at small increase of ϕ_{P0} and then exhibits an approximate linear increase with ϕ_{P0}. Theoretically, ϕ_{P0} could be arbitrarily determined for adjustable stiffness of the system under the permissible source supply of the system. In practice, it is preferred to employ $\phi_{P0} \le 4$ for achieving both fairly large adjustable stiffness and remaining a moderate pressure variation for energy saving effect.

(2) Variable height adjustment

The additional pressure ratio ϕ_{P0} can also be utilized to adjust the isolator height when ϕ_{P0} and ϕ_{KP} are properly set [3]. The required ϕ_{P0} for approaching height limitation ($-\alpha\phi_L \le \phi_{xp0} = x_{p0}/\hat{x}_{b0} \le \alpha\phi_L$ ($0 \le \alpha \le 1-1/\phi_L$)) is calculated according to the static equilibrium for the non-dimensional static displacement from Eq.(1).

$$(1-\frac{\alpha}{2})^{\lambda}[1+s_{u2}\phi_{KP2}(\frac{1}{1+\alpha/\phi_{KL2}})^{\lambda}]-1 \le \phi_{P01} \le (1+\frac{\alpha}{2})^{\lambda}[1+s_{u2}\phi_{KP2}(\frac{1}{1-\alpha/\phi_{KL2}})^{\lambda}]-1 \qquad (6)$$

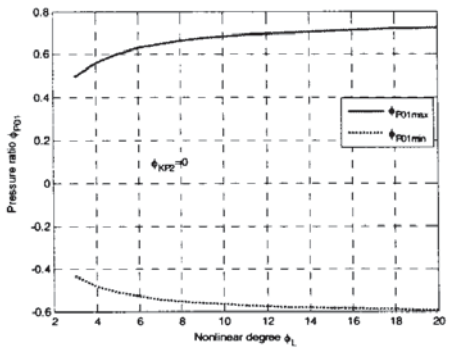

(a) $\phi_{KP} = 0$

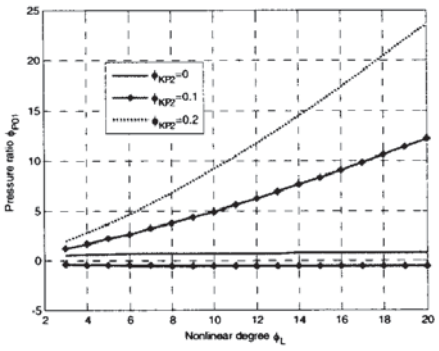

(b) $\phi_{KP} > 0$

Fig 6 Required additional pressure ratio for height limitation with different ϕ_{KP2}

Fig. 6 shows the required ϕ_{P0} for height limitation under different ϕ_L with $\phi_{KP} = 0$ and $\phi_{KP} > 0$ when specifying $\alpha = 1-1/\phi_L$. As seen from Fig.6a, the required ϕ_{P0} for height limitation is significantly dependent on small ϕ_L and slightly dependent on large ϕ_L for single-working-chamber pneumatic spring ($\phi_{KP} = 0$). And the required ϕ_{P0} for height limitation is usually not large at any ϕ_L, which indicates that the variable height adjustment with efficient utilization of air volume could be easily obtained in practical application. On the other hand, the required ϕ_{P0} for maximum height is greatly increased with ϕ_{KP} (red line) while the required ϕ_{P0} for minimum height is slightly increased with ϕ_{KP} (blue line) when $\phi_{KP} > 0$, as seen from Fig 6b. This indicates that the maximum height for fully space utilization of the dual-working-chamber with large initial volume is hard to be approached due to the resistance effect of counter pressure in height control. Noticeably, ϕ_{P0} and ϕ_{KP}

for variable height control is usually not larger than the permissible ϕ_{P0} for variable stiffness control in case of compact design with small ϕ_L.

3.1.5 Specification of ξ_2 and ϕ_{DVMR} for MR damping

According to the non-dimensional dynamic model for MR damper element, four important design parameters (e.g. passive damping ratio, dynamic range, velocity-dependent and position-dependent factor) are used to characterize majority performance capability of the MR valve [3]. The frequency range for justifying the effective isolation range is set as $\omega_n \sim 10\omega_n$ since the transmissibility at fairly high frequency is naturally very small and has no significant meaning for isolation evaluation. On one hand, small passive damping ratio ξ_2 is necessary for fast vibration mitigation using semi-active control. It is noted that the decaying velocity of the transmissibility of the MrEPI at frequency $\omega_n \sim 10\omega_n$ is almost the same as the that of semi-active isolator using ideal sky-hook (-40db) if $\xi_2 \le 0.035$. As such, ξ_2 is required to be less than 0.035 for guaranteeing fast vibration mitigation at high frequency when using semi-active control for the MrEPI. On the other hand, it is concluded from simulation that the dynamic range ϕ_{DVMR} with certain small ξ_2 should be as large as possible for effective resonance attenuation in vibration control process. In addition, large velocity-dependent and small position-dependent factor should be used for less hysteresis behavior, which means that the time constant of the MR valve should be designed as small as possible for favorable dynamic control [3,8].

3.2 Component level design

The component level design is conducted for determining the optimal geometric and material configuration of the MR valve based on the parameter requirements (e.g. required small passive damping ratio, time constant and maximizing dynamic range) from system level design of the MrEPI.

3.2.1 Schematic structure and non-dimensional analytical model of MR valve

Different from [10], the schematic structure of the MR valve with annular resistance flow channel used for the MrEPI is show in Fig 7. The electromagnetic coil wound around a nonmagnetic coil bobbin is placed between the magnetic outer housing and the magnetic core vale, which results in separate coil wire from the annular duct full of MR fluids for easy wire protect. The detailed damping force could refer to [3]. The damper capacity, which could be evaluated by several performance index such as dynamic range, passive damping ratio, time constant etc., could be formulated in terms of deliberately defined input non-dimensional variables (Table1) according to analytical models.

$$\begin{cases} \phi_{DVMR} = \dfrac{F_\tau}{F_\eta} = \dfrac{f_c}{12(\Delta_{p1} + \Delta_{p2}/\phi_{La})} \dfrac{\phi_r}{\phi_{Apd}} \dfrac{\tau_y(H_{MR})}{\eta} \phi_{gr} \dfrac{r_0}{v_p} \\ \xi_2 = \dfrac{c_{vis}}{2\sqrt{mk_0}} = 12\pi n(\Delta_{p1}\phi_{La} + \Delta_{p2}) \dfrac{\phi_{Apd}}{\phi_r^2} \phi_{E1}\phi_{gr} \\ F_\tau = \pi r^2 \Delta P = 2nf_c \dfrac{\tau_y(H_{MR})}{\phi_r} \phi_{La}\phi_{gr}{}^2 \pi r_0{}^2 \\ T_{in} = \Delta_5[(\Delta_{H1} + \phi_{M1})\phi_{La} - \Delta_{H2}\phi_{La}{}^2]\phi_{gr}{}^2 \dfrac{r_0^2}{r_{w1}} \end{cases} \tag{7}$$

Where, $\Delta_{p1} = 1 - \dfrac{1}{k_d{}^3}$, $\Delta_{p2} = \dfrac{\phi_{LP}}{2n}\dfrac{1}{k_d{}^3} + \dfrac{2}{3n}\phi_p\phi_{rRd}\phi_r{}^3$, $\phi_{Apd} = \dfrac{A_p}{A_d} = \dfrac{1}{2\phi_{rRd}\phi_r}$, $\Delta_5 = \mu_0\mu_{MR}\dfrac{\phi_{rRd}}{\phi_{rdc}}$,

$\Delta_{H1} = \dfrac{\phi_{rwc}}{\phi_r}[\dfrac{\phi_{LP}}{n} - 2k_{b1}\phi_r]$, $\Delta_{H2} = \dfrac{2\phi_{rwc}}{\phi_r}$, $\phi_{rRd} = \dfrac{\bar{R}_d}{r} = \phi_{r4} - \phi_{r3} - \dfrac{1}{2}\phi_r - (\phi_{rwc} + k_{b1}\phi_r + k_{b2}\phi_r)$,

$\phi_{rdc} = \dfrac{\bar{d}_c}{r} = 2\phi_{r1} + \phi_{rwc} + 2k_{b1}\phi_r + 2k_d\phi_r$, $\phi_{rwc} = \dfrac{w_c}{r} = \phi_{r4} - \phi_{r3} - \phi_{r1} - k_d\phi_r - k_{b1}\phi_r - k_{b2}\phi_r$.

Table 1 Definitions of input non-dimensional variables for MR valve

Non-dimensional variables		Definitions
Geometry relevant variables	Normal geometry variable	$\phi_r = \frac{t_d}{r}$ $\phi_{r1} = \frac{R_c}{r}$ $\phi_{r3} = \frac{t_h}{r}$, $\phi_{r4} = \frac{R}{r}$, $\phi_{LP} = \frac{L}{r}$, $\phi_{La} = \frac{L_a}{r}$, $\phi_{r0} = \frac{r}{r_0}$
	Tubing geometry variable	$\phi_p = \frac{L_t}{r}\frac{r^4}{r_t^4}$
	Additional geometry variable	$k_d = \frac{t_{d1}}{t_d}$, $k_{b1} = \frac{t_{b1}}{t_d}$, $k_{b2} = \frac{t_{b2}}{t_d}$
Material relevant variable		$\phi_{M1} = \frac{B_{sat}}{\mu_0 \mu_{MR} H_{MRsat}}$, $\phi_{M2} = \frac{H_{MRsat}}{r_0 I/(2A_w)}$,
Exciting relevant variable		$\phi_{E1} = \frac{\eta r_0}{m\omega_n}$

Note: B_{sat} is the saturation of magnetic material used for MR valve including valve core, magnetic pole, and outer housing etc. H_{MRsat}, μ_{MR} are the saturated magnetic intensity and relative permeability of MR fluids, respectively. A_w is the cross sectional areal copper coil. A_d is the cross-sectional area of the annular gap given by $A_d = wt_d$, $\bar{d}_c$ is the average diameter of the coil, r_0 is the reference cylinder radius of MR damper. I is the applied current, $\mu_0 = 4\pi \times 10^{-7}$, $v_p = \hat{x}_{b0}\sqrt{k_0/m}$ and $\omega_n = \sqrt{k_0/m}$.

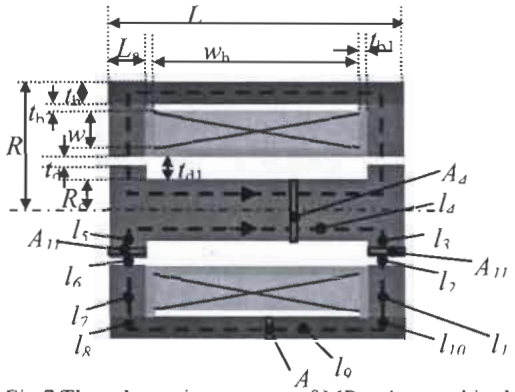

Fig 7 The schematic structure of MR valve used in the MrEPI

3.2.2 Analytical method for optimal design of MR valves

In view of large amount of design parameters with coupling effect for characterizing the conflict performance index, parameter optimization is necessary in design of the MR valve. Generally, a multi-objective function is employed in literature [9]. However, the weight factor in multi-objective function is usually empirically specified and has no clear regulation. As a result, different weight factors will cause significant different damper capacity and consequently greatly influence the achievable performance in semi-active vibration control. Therefore, a new analytical method- optimization method with preset index- for the MR valve is proposed, which maximizes achievable active drop pressure or damping force while fulfills worst-case requirements of preset index such as passive damping ratio and time constant for obtaining optimal internal design parameters.

Refer to the structure of the MR valve in Fig.7, The magnetic flux conservation rule of the circuit in some critical section area is given as follows according to Gauss's Law [10]

$$\Phi = B_{11}A_{11} = B_9 A_9 = B_4 A_4 = B_{MR}A_{MR} \tag{8}$$

Where, $A_{11} = 2\pi R_c L_a$, $A_9 = \pi[R^2 - (R - t_h)^2]$, $A_4 = \pi R_c^2$, $A_{MR} = 2\pi \bar{R}_d L_a$.

The active length ratio ϕ_{La} would be tentatively synthesized in terms of specified variables considering practical constraints such as saturation constraint of magnetic material and MR fluid, preset index, and high efficient usage of geometric volume etc.. And then the optimal ϕ_{La} and other internal design variables could be specified for maximizing pressure drop of the MR valve.

Step 1: Specify the reference radius of MR damper cylinder r_0, required reference passive damping ratio ξ_{ref} and non-dimensional time constant T_{inref} according to the system level design and select a type of MR fluid. Specify external design parameters including geometry relevant variables ϕ_{r4}, $\phi_{LP}, k_d, k_{b1}, k_{b2}, \phi_p$ material relevant parameters ϕ_{M2} and exciting relevant variable ϕ_{E1} as shown in Table 1.

Step 2: Select initial values for internal non-dimensional design parameters ϕ_r and ϕ_{r3}.

Step 3: Calculate the valve core ratio through assuming that $B_4 = B_9 > B_{11}$ in Eq. (8)

$$\phi_{r1} = \sqrt{(2\phi_{r4} - \phi_{r3})\phi_{r3}} \quad \text{and} \quad \phi_{La} \geq 0.5\phi_{r1} \tag{9}$$

Step 4: Derive the permissible value of ϕ_{La} according to practical constraints

On one hand, ϕ_{La} is constrained by magnetic saturation of the magnetic material used in the MR valve, such that,

$$B_{11} = \frac{B_{MR} 2\pi \bar{R}_d L_a}{2\pi R_c L_a} = \frac{\mu_0 \mu_{MR} \phi_{rRd}}{\phi_{r1}} [\frac{Ir}{2A_w}(\Delta_{H1} - \Delta_{H2}\phi_{La}) + H_{MR0}] \leq B_{sat} \tag{10a}$$

$$B_4 = \frac{B_{MR} 2\pi \bar{R}_d L_a}{\pi R_c^2} = \frac{2\mu_0 \mu_{MR} \phi_{rRd}}{\phi_{r1}^2} [\frac{Ir}{2A_w}(\Delta_{H1} - \Delta_{H2}\phi_{La}) + H_{MR0}]\phi_{La} \leq B_{sat}, \tag{10b}$$

$$B_9 = \frac{B_{MR} 2\pi \bar{R}_d L_a}{\pi[R^2 - (R - t_h)^2]} = \frac{2\phi_{rRd}}{2\phi_{r4}\phi_{r3} - \phi_{r3}^2} \mu_0 \mu_{MR} [\frac{Ir}{2A_w}(\Delta_{H1} - \Delta_{H2}\phi_{La}) + H_{MR0}]\phi_{La} \leq B_{sat} \tag{10c}$$

In addition, the applied magnetic field intensify should not be too large for preventing the MR fluids from operating in a saturated yield stress resulting in less sensitivity in control.

$$0 < H_{MR} = \frac{Ir}{2A_w}(\Delta_{H1} - \Delta_{H2}\phi_{La}) \leq H_{MRsat} \tag{10d}$$

On the other hand, the preset index (e.g., small passive damping ratio and time constant) are added into the optimization process for non-deteriorated performance in vibration control due to unsophisticated weight selection. The constraints for non-dimensional variables ξ_2 and ϕ_{Tin} is given by

$$\xi_2 = 12\pi n(\Delta_{p1}\phi_{La} + \Delta_{p2})\frac{\phi_{Apd}}{\phi_r^2}\phi_{E1}\phi_{gr} \leq \xi_{ref}, \tag{11a}$$

$$\phi_{Tin} = \frac{T_{in}}{r_0^2 / r_{wl}} = \Delta_5[(\Delta_{H1} + \Delta_{M1})\phi_{La} - \Delta_{H2}\phi_{La}^2]\phi_{gr}^2 \leq \phi_{Tinref}, \tag{11b}$$

Combining Eq(10) and Eq(11), the available range of ϕ_{La} could be specified and the achievable damper performance is calculated according to Eq(7) with a minimum ϕ_{La} in view of minimum active length of magnetic pole.

Step 5: Chose new values of non-dimensional values ϕ_r and ϕ_{r3} with certain incensement, repeat Step 2-4 until finding the maximum pressure drop.

3.2.3 Optimization results

Fig.8 shows the achievable performance under different external design parameters ϕ_{r4} and ϕ_{LP} using the proposed optimization method with preset index. As seen, the achievable passive damping ratio and time constant are always below reference values as expected whenever different design parameters. That is, the small passive damping ratio and time constant could be guaranteed for achieving satisfactory isolation performance at high frequency and good dynamic response, and at the same time the active damping force is maximized for effectively reducing the resonance peak. Furthermore, it is noted from Fig.8 that there is no solution for some design parameters (e.g. $\phi_{LP} < 1$) due to constraint of preset index and other geometric and material constraints in optimization. It is obviously noticeable that the appropriate total length of MR valve for compact volume design could be obtained at $\phi_{LP} = 1.5 \sim 2.5$, and $\phi_{r4} = 1.5 \sim 2$ since dramatically improved performance could be obtained in this zone. The other external design parameters upon achievable performance can be extensively analyzed in similar way. In a word, the proposed optimization method with preset index based on non-dimensional analytical formulations for component level design of MR valve in the MrEPI removes the dilemma of empirically selecting appropriate weight in conventional optimization method and facilitate for

sensitivity analysis in synthesizing appropriate design parameters.

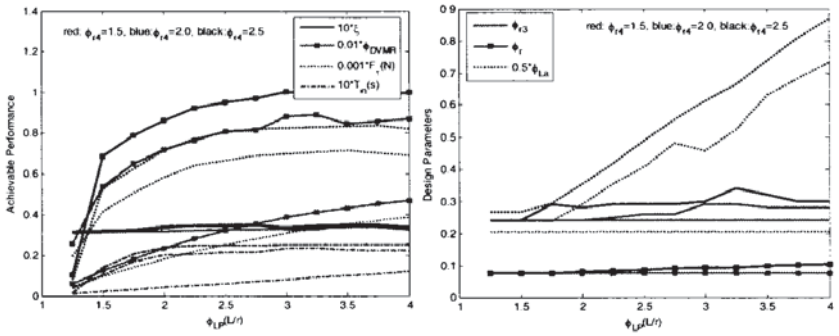

Fig8 The achievable performance of and optimized geometry parameters of the MR valve

3.3 Dimensional realization

Next, the optimal non-dimensional parameters synthesized above could be dimensioned according to practical application requirements for the actual plant system. To illustrate clearly, the input data from practical application requirements, the appropriate non-dimensional design parameters (DVs) from system level design and component level design, and the calculation for dimensional realization are shown in Table 2.

Table 2 Dimensional realization for actual plant system

Input data for practical system	Appropriate DVs	Calculation for dimensional realization
$\hat{x}_{b0}, \omega_{n0}, m_r, P_s$	$\phi_L \geq 3$, $\xi_3 \approx 0.25$, $0 \leq \phi_{P01} \leq 4$, $0 \leq \phi_{V01} \leq 4 \sim 5$	$L_{u0} = L_{d0} = L_{au} = \phi_L \hat{x}_{b0}$, $P_{dr} = \frac{P_s + P_{atm}}{\Delta p(\phi_L)} \frac{1}{\phi_{P01}}$, $A_d \geq \frac{m_r g - s_u P_{atm} A_u}{P_{dr} - P_{atm}}$,
Selection of coil wire and MR fluid	$\phi_{r4} = 1.5 \sim 2.5$, $\phi_{LP} = 1.5 \sim 2.5$	$r = \phi_{gr} r_0$, $R = r\phi_{r4}$, $L = r\phi_{LP}$, $m = r_0 \eta / (\omega_{n0} \phi_{E1})$, $I_{max} = 2A_w H_{MRsat} / (r_0 \phi_{M2})$, $r_t = (L_t r^3 / \phi_P)^{1/4}$, $B_{sat} = \phi_{M1} \mu_0 \mu_{MR} H_{MRsat}$,

Note: L_{u0}, L_{d0} and L_{au} are the effective initial length of the upper, lower and auxiliary pneumatic chamber, respectively, P_s and P_{dr} are relative pressure of source supply and the initial pressure of lower chamber, respectively. $\Delta p(\phi_L)$ is the maximum pressure variation dependent on ϕ_L seen from Fig 5.

4 Achievable Isolation Performance for the optimally designed MrEPI

Fig 9 shows the isolation performance (acceleration transmissibility and relative displacement) of the MrEPI with independently adjustable stiffness and damping under different stiffness level dependent on ϕ_{P0} or ϕ_{V0} ($0 \leq \phi_{P01} \leq 3, 0 \leq \phi_{V01} \leq 4$) using sky-hook controller as in [12] with $\xi_2 = 0.033$, $\phi_{DVMR} = 78.5$. The theoretical stiffness adjustment could be calculated from $k_s = 1/6$ ($\phi_{V01} = 4$) to $k_s = 5$ ($\phi_{P01} = 3$) according to Eq.(5), and could be verified from natural frequency seen from Fig.9. As seen, good isolation performance with effective resonance attenuation and fast mitigation at high-frequency under both low and high stiffness can be achieved owning to fairly small passive damping ratio being guaranteed and large active damping force being optimized for the MrEPI.

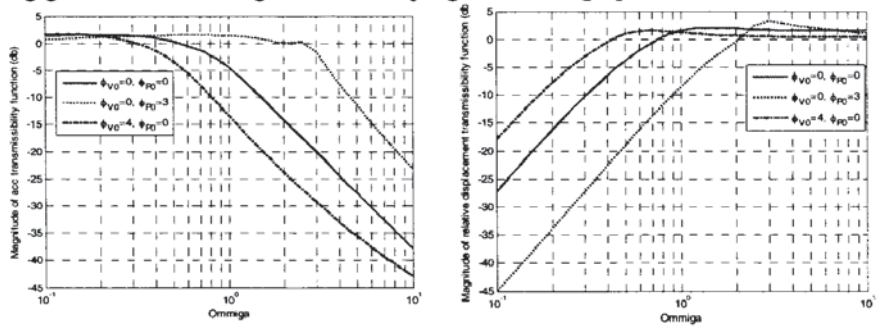

Fig.9 The isolation performance of the MrEPI with different stiffness level dependent on ϕ_{P0} or ϕ_{V0}

5. Conclusions

An effective non-dimensional analytical method for optimal design of a MrEPI is developed with the consideration of practical constraints. The design problem is to find the appropriate geometry dimensions and material configuration of the MrEPI for maximizing stiffness and damping adjustment as well as beneficial vibration control of the isolator through analyzing the significant influence of design parameters upon the achievable performance. The design is accomplished through three levels: system level design of pneumatic spring and MR damping element, component level optimal design of MR valve with non-dimensional internal design parameters, and dimensional realization level design for actual plant system according to practical application requirements. In addition, the simulation results demonstrated good acceleration and relative displacement transmissibility for the optimally designed MrEPI using semi-active sky-hook controller.

References

(1) H. V. Deo, N. P. Suh, Variable stiffness and variable ride-height suspension system and application to improved vehicle dynamics, SAE World Congress Detroit, Michigan, 2005
(2) E. Guglielmino, T. Sireteanu, C.W. Stammers, G. Ghita, M. Giuclea, Semi-active suspension control, improved vehicle ride and road friendliness, 1st Edition., Springer, 2008
(3) X. C. Zhu, X. J. Jing, L. Cheng. A magnetorheological fluid embedded pneumatic vibration isolator allowing independently adjustable stiffness and damping. Smart Mater. Struct. 20 (2011) 085025 (18pp)
(4) P. Anusonti-Inthra, Semi-active control of helicopter vibration using controllable stiffness and damping devices, Dotor Thesis, The Pennsylvania State University, 2002
(5) G. Quaglia, M. Sorli, Air suspension dimensionless analysis and design procedure. Vehicle system design, Volume 35 (6), 2001, pp: 443-475
(6) J. H. Lee, K. J. Kim, A method of transmissibility design for dual-chamber pneumatic vibration isolator. Journal of Sound and Vibration, Volume 323, 2009, pp: 67-92
(7) J. H. Moon, B. G. Lee. Modeling and sensitivity analysis of a pneumatic vibration isolation system with two air chambers, Mechanism and Machine Theory, Volume 45, 2010, pp: 1828-1850.
(8) H. Gavin, J. Hoagg, M. Dobossy. Optimal design of MR dampers, Proc. U.S.-Japan Workshop on Smart Structures for Improved Seismic Performance in Urban Regions, Seattle WA, 2001, pp: 225-236.
(9) Q.H. Nguyen, S.B. Choi. Optimal design of a vehicle magnetorheological damper considering the damping force and dynamic range, Smart Mater. Struct. Volume 18, 2009, 015013 (10pp).
(10) Q H Nguyen, S B Choi, Y S Lee, M S Han. An analytical method for optimal design of MR valve structures, Smart Mater. Struct. , Volume 18, 2009, 095032 (12pp).
(11) G. J. Hiemenz, W. Hu, N. M. Wereley, Semi-active magnetorheological helicopter crew seat suspension for vibration isolation, Journal of Aircraft, Volume 45(3), 2008, pp: 945-953
(12) Y. T. Choi, N M Wereley, Mitigation of biodynamic response to vibratory and blast-induced shock loads using magnetorheological seat suspensions, Proc. IMechE Volume 219 Part D: J. Automobile Engineering, 2005, pp: 741-753
(13) L. Pang, G. M. Kamath, N. M. Wereley. Analysis and testing of a linear stroke magnetorheological damper, AIAA/ASME/AHS Adaptive Structures Forum, Long Beach CA, 1998, pp. 2841-2856.

Acknowledgements

The authors would like to acknowledge the support from the GRF project (Ref 517810) of Hong Kong RGC, Department General Research Funds and Competitive Research Grants of Hong Kong Polytechnic University. Xiaocong Zhu would also like to acknowledge the support from a NSF project of China (Grant No. 50905156).